SPECIAL ISSUE
Basic Plasma Processes in Solar-Terrestrial Activities

April 2012 Vol.57 No.12: 1405–1408
doi: 10.1007/s11434-011-4913-1

An interpretation of density holes observed by Cluster and Double Star in solar wind

QURESHI M N S[1,2], SHI JianKui[1*], CHENG ZhengWei[1] & LIU ZhengXing[1]

[1] *State Key Laboratory of Space Weather, Center for Space Science and Applied Research, Chinese Academy of Sciences, Beijing 100190, China;*
[2] *Department of Physics, GC University, Lahore 54000, Pakistan*

Received September 6, 2011; accepted November 3, 2011; published online February 21, 2012

To interpret density holes in the solar wind, which are nonlinear structures observed by Cluster and Double Star, we propose an electrostatic ion fluid model. We derive the Sagdeev potential from the magnetohydrodynamic (MHD) equations and study the characteristics of nonlinear structures in our model. The results show that density depletions (or holes) can develop from linear ion acoustic waves or ion cyclotron waves in space plasmas when parameters such as Mach number, initial electric field and ratio of ion to electron temperature satisfy certain conditions. In our model, the relative density depletion (or density holes) is from 0 to 1, and the time duration of density holes is from 2 s to more than 98 s. These are in good agreement with the observations by Cluster and Double Star in the solar wind. Our model also shows that the density holes should be accompanied by bipolar electric field solitary structures, which have also been observed by Cluster in the solar wind.

ion density hole, solar wind, Cluster and Double Star observations, theoretic interpretation

Citation: Qureshi M N S, Shi J K, Cheng Z W, et al. An interpretation of density holes observed by Cluster and Double Star in solar wind. Chin Sci Bull, 2012, 57: 1405–1408, doi: 10.1007/s11434-011-4913-1

Nonlinear waves in space plasmas have been observed by various satellites, such as S3-3, Viking, Polar, Fast, Geotail and Cluster in areas such as the upper ionosphere, auroral field lines, magnetopause, magnetosheath and so on [1–7]. The Cluster and Double Star satellites recently observed plasma density holes upstream of the Earth's collisionless bow shock at apogee distance of about 19 and 13 Earth radii, respectively [8]. During six Cluster orbits in 2003 and 2005, 146 density holes were observed upstream of the Earth's bow shock with a mean duration of 17.9±10.4 seconds and a mean relative density depletion of 0.69±0.15. Density holes observed on March 2, 2005 by both Cluster and Double Star have also been analyzed in detail by Parks et al. [8].

Figure 1 shows typical examples of density holes observed by Cluster on March 2, 2005 and March 1, 2003 from different bow shock crossings near the subsolar region [8]. These holes have symmetric shapes with density elevated on both sides or only on one side from the background density. Density holes have also been observed by Cluster C1 and C3 upstream of the Earth's bow shock with mean durations of 32.0±20.2 seconds (for C1) and 27.9±13.5 seconds (for C3), and with mean relative density depletions of 10.1±12.2 (for C1) and 7.7±8.1 (for C3). We can see that the density dips (the ratio of maximum to minimum) can be more than 20 times [9].

Various theoretical studies have been proposed to interpret nonlinear waves with different plasma models ranging from weakly nonlinear to fully nonlinear theories. Washimi and Tanuity [10] did the first study on ion acoustic solitary waves using the Kortweg-de Vries (KdV) equation with a fluid model. Later, ion acoustic density solitons were studied using the fully nonlinear Sagdeev potential developed by different authors [11–14]. All of the theoretical works mentioned above are on ion acoustic solitary waves under the special conditions in space plasmas. Wu et al. [15–17] proposed a model and obtained analytic solutions of finite-

*Corresponding author (email: jkshi@cssar.ac.cn)

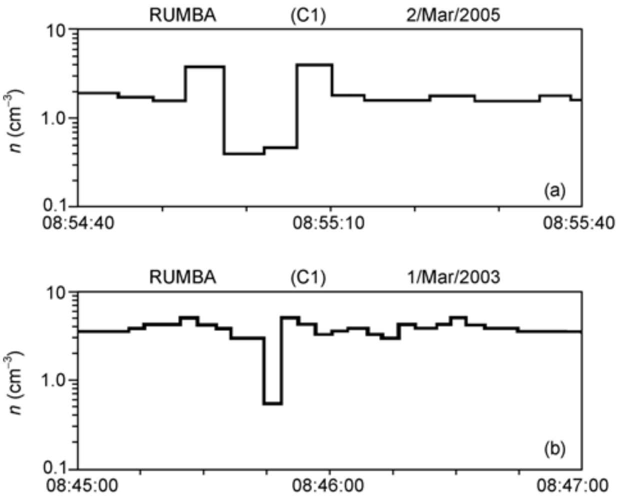

Figure 1 Typical examples of ion density holes observed by Cluster on March 2, 2005 with density overshoot on both edges (a) and on March 1, 2003 with overshoot from the background value on one side (b) [8].

amplitude solitary kinetic Alfvén waves. They also theoretically studied solitary kinetic Alfven waves with the two-fluid model. The relevant phenomenon in the solar wind has been studied by various authors [18–20]. However, so far no model has been proposed for the ion density depletion structures (density holes) observed by Cluster and Double Star in the solar wind region.

To interpret the density holes observed by Cluster and Double Star in the solar wind region, we propose a magnetohydrodynamic (MHD) model in which the Sagdeev potential is strictly derived from the MHD equations in magnetized plasma for the field-aligned waves. In our model, the density depletion as a numeric solution can be obtained under a certain plasma condition, and the model results are consistent with the Cluster observations.

1 Theoretical formulism and solution

We assume that the fluid consists of electrons and ions, and that the magnetic field is in the z-direction. The phase velocity v_p lies between the electron and ion thermal velocities so that the Landau damping can be neglected. The wave scale $\lambda >> \lambda_D$ (λ_D is the Debye radius), so that charge separation effects can be neglected and the quasi-neutrality condition may be applied, i.e. $n \approx n_e \approx n_i$. Here n is the particle number density, and n_e and n_i are the electron and ion number densities, respectively.

Using cylindrical coordinates and neglecting electron inertia, the MHD equations for the ions can be written as

$$\frac{\partial n}{\partial t}+\frac{\partial (nv_r)}{\partial r}+\frac{\partial (nv_z)}{\partial z}=-\frac{nv_r}{r}, \tag{1}$$

$$\frac{\partial v_r}{\partial t}+v_r\frac{\partial v_r}{\partial r}+v_z\frac{\partial v_r}{\partial z}=-\frac{1}{m_i n}\frac{\partial p}{\partial r}-\frac{e}{m_i}\frac{\partial \varphi}{\partial r}+\frac{v_\theta^2}{r}+\varOmega_i v_\theta, \tag{2}$$

$$\frac{\partial v_\theta}{\partial t}+v_r\frac{\partial v_\theta}{\partial r}+v_z\frac{\partial v_\theta}{\partial z}=-\frac{v_r v_\theta}{r}-\varOmega_i v_r, \tag{3}$$

and

$$\frac{\partial v_z}{\partial t}+v_r\frac{\partial v_z}{\partial r}+v_z\frac{\partial v_z}{\partial z}=-\frac{1}{m_i n}\frac{\partial p}{\partial z}-\frac{e}{m_i}\frac{\partial \varphi}{\partial z}, \tag{4}$$

with

$$p=nT_i, \tag{5}$$

and

$$n=n_i\approx n_e\approx n_0\exp(e\varphi/T_e), \tag{6}$$

where p is the thermal pressure, e is the elementary charge, φ is the electric potential, v is the ion velocity, n_0 is the background number density, and T_i and T_e are the ion and electron thermal energy, respectively. After linearizing eqs. (1)–(4), we obtain the linear dispersion relation $\omega^2(\omega^2-ac_s^2k^2)\times(\omega^2-\varOmega_i^2)=0$. Here ω is the wave frequency, $\varOmega_i=eB_0/(m_i c)$ is the ion cyclotron frequency, $c_s=(T_e/m_i)^{1/2}$ is the ion acoustic velocity, and $a-1=T_i/T_e$ is the ratio of the ion and electron temperatures. The linear dispersion relation shows that the disturbances in the linear level are ion acoustic waves and ion cyclotron waves.

We normalized the above eqs. (1)–(6) and shifted to a co-moving frame using the variable

$$S=(k_r r+k_z z-\omega t)\varOmega_i/\omega=(\alpha R+\gamma Z-\tau M)/M. \tag{7}$$

Employing the standard algebraic techniques and using the boundary conditions $N|_{s=0}=1$ and $V|_{s=0}=0$, we obtain eq. (8) for parallel wave propagation:

$$\frac{1}{2}\left(\frac{\mathrm{d}N}{\mathrm{d}S}\right)^2+\varPsi(N)=0, \tag{8}$$

where

$$\varPsi(N)=\frac{\left[\left(N\sqrt{1-\frac{2a}{M^2}\ln N}-1\right)^2-\left(\frac{a}{M^2}-1\right)^2E_0^2\right]\left(N\sqrt{1-\frac{2a}{M^2}\ln N}\right)^2}{2\left[\frac{a}{M^2}-\left(1-\frac{2a}{M^2}\ln N\right)\right]^2}. \tag{9}$$

Here E_0 is the initial value of the electric field E. In eqs. (7)–(9), the dimensionless quantities are $N=n/n_0$, $\tau=\varOmega_i t$, $R=r/\rho_i$ (where ρ_i is the ion gyroradius), $Z=z/\rho_i$, $V=v/c_s$, $\varPhi=e\varphi/T_e$ and the Mach number $M=v_p/c_s$. Also, k_z is the component of $\boldsymbol{k}$ in the z-direction, and $\gamma=1$ for parallel propagation.

From eqs. (8) and (9) we see that there will be solutions only for the "Sagdeev potential" $\varPsi(N)<0$. By analyzing the properties of the Sagdeev potential $\varPsi(N)$, we can find the solutions for ion density depletion when the plasma parameters satisfy the condition

$$\left|\left(a/M^2-1\right)E_0\right|=1,\quad a/M^2>1,\quad G_m>2. \tag{10}$$

Here,

$$G_m=\sqrt{a/M^2}\exp\left[\left(1-a/M^2\right)/\left(2a/M^2\right)\right]. \tag{11}$$

Indeed, if the condition (10) is satisfied, there will be two dimensionless particle number densities N_1 and N_2 obeying $0<N_1<1<N_2$ and $\Psi(N)<0$ for $N_1<N<N_2$, where $\Psi(N)$ has the properties $\Psi(N_1)=0$, $\Psi(N_2)=0$, $\Psi'(N_1)<0$ and $\Psi'(N_2)=0$. If so, the profiles of $\Psi(N)$ will be those shown in Figure 2, i.e. $\Psi(N)$ is decreasing at $N=N_1$ and has a maximum at $N=N_2$. Then, eq. (8) has a solution corresponding to ion density depletion. Therefore, eq. (10) is the condition for existence of an ion density depletion or density hole.

Figure 3 plots density structures corresponding to the $\Psi(N)$ profiles in Figure 2. Each of these curves shows a density depletion or density hole in the space plasma that satisfies the condition (10) in our model. We see that the dip in the density depletions increases when both M and E_0 increase in a particular combination. The density dips in Figure 3 are 0.356 for curve (a), 0.275 for curve (b), and 0.234 for curve (c). Furthermore, the depletions (holes) in Figure 3 also have overshoots in density from the background value on both edges. The overshoots are about 0.5 for all three depletions but a little different for each case.

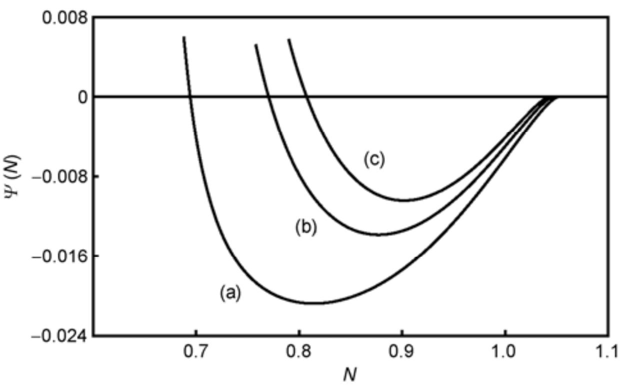

Figure 2 Sagdeev potential profiles for different parameter values satisfying the condition (10) for (a) $a/M^2=10$ and $E_0=1/10$, (b) $a/M^2=11$ and $E_0=1/11$, and (c) $a/M^2=12$ and $E_0=1/12$.

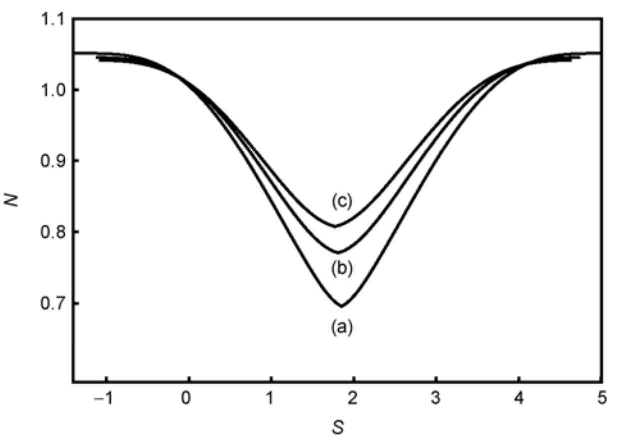

Figure 3 Density depletion structures corresponding to the Sagdeev potential profiles in Figure 2. The curves (a), (b) and (c) correspond to the curves (a), (b) and (c) in Figure 2, respectively.

Figures 2 and 3 just give typical examples of the Sagdeev potential and the corresponding density depletion structures for the condition (10). They show that from our model an electrostatic density depletion can exist in geo-space plasmas when the plasma parameters, such as Mach number M, ion-to-electron temperature ratio a–1, and initial electric field E_0 satisfy the condition (10).

2 Comparison with observation and discussion

From our model results, we can obtain the nonlinear density structures corresponding to ion density depletions or holes when the condition (10) is satisfied. The structures are consistent with the Cluster and Double Star observations. We can further compare our model results to the observations.

In Cluster observations, ion density holes upstream of the Earth's bow shock have relative values from 0.2 to 0.9 with duration from 4 to 45 s. The reported ion gyro-frequency values and local ion acoustic speeds from that region are $f_{gi}\approx 0.08$ Hz and 90 km/s, respectively [8]. Density holes in the same region have also been observed by Cluster with slightly longer durations ranging from 12 to 52 s and larger relative density depletions ranging from 0.5 to 0.95 inside the holes [9]. If we consider $a/M^2>1$ in our model, then according to eq. (9) and condition (10), N_1 varies from 0 to 1. However, N_1 cannot be zero physically or 1 for a depletion. Moreover, if we consider $S=2-10$ and the observed ion gyro-frequency $f_{gi}\approx 0.08$ Hz in our model, the time duration of the depletion would be from 2 to more than 98 s. Therefore, our model can also interpret the density depletion and hole duration observed by Cluster.

Some ion holes in the Cluster observation have density overshoots from the background value on both edges (Figure 1(a)), and some have overshoots on one side (Figure 1(b)) [8]. In our model, all ion holes have overshoots from the background value on both edges. Indeed, from Figure 1(b), if we consider a longer duration or wider structure, it seems that the hole from Cluster's observation on March 1, 2003 also had a density overshoot from the background value on both edges.

By normalizing eq. (6) we can obtain the electric field as $E=-1/N\cdot dN/dS$. Using eq. (8), the electric field can be written as $E=\mp\sqrt{-\frac{2}{N}\Psi(N)}$. For example, the electric field corresponding to the density depletion in Figure 3 should be a bipolar structure. This is important to understand the physical process of the ion density holes. At first, some linear disturbances gradually develop up to the nonlinear level with the gradually developing electric field, which enhances the density disturbance. Finally, bipolar electric field structures (EFSs) are formed as density holes. The bipolar EFSs were also observed by Cluster in the solar wind [21,22]. Hobara et al. [22] discussed the role of bipolar EFSs. They consider that the bipolar EFSs are responsible for the heating of space plasma and accelerating charged particles near the Earth's bow shock and are isolated electric field pulses showing nonlinear behavior in the electric field waveform.

3 Conclusion

Density holes have been observed by Cluster and Double Star in the solar wind upstream of the Earth's bow shock. The relative density depletion in the holes ranges from 0.2 to 0.95, and the duration of each hole ranges from 4 to 52 s. To interpret the characteristics of the density holes (such as the density depletion and its duration), we presented an MHD model in a magnetized plasma for the wave propagation along the magnetic field. We derived the Sagdeev potential from our model equations and obtained ion density depletions (holes) under certain plasma conditions. The ion density depletion (or hole) can develop from a linear ion acoustic wave or ion cyclotron wave in space plasma. The results from our model show that the relative density depletion could be from 0 to 1 and that the time duration of the density holes can be from 2 to more than 98 s in the solar wind. These are consistent with the Cluster observations. We can also obtain bipolar electric field structures from our model corresponding to ion density depletions.

Therefore, our MHD model can be used to interpret some properties of the ion density holes in the solar wind observed by Cluster and Double Star. However, we should note that, in the Cluster observations, the density depletion can have a density overshoot from the background on both edges or on only one side. In our model, all the density depletions have overshoots from the background on both edges of the hole. However, if we prolong the duration of the ion density depletions or holes observed by Cluster in the solar wind, the depletions or holes will also have density overshoots from the background on both edges. This needs to be further studied.

This work was supported by the National Natural Science Foundation of China (41074114, 40921063, 40804031) and the Specialized Research Fund for State Key Laboratories of China.

1 Temerin M, Cerney K, Lotko W, et al. Observations of double layers and solitary waves in the auroral plasma. Phys Rev Lett, 1982, 48: 1175–1179
2 Bostrom R, Gustafsson G, Holback B, et al. Characyeristics of solitary waves and weak double layers in the magnetospheric plasma. Phys Rev Lett, 1988, 61: 82–85
3 Mozer F S, Ergun E, Temerin M, et al. New features of time domain electric-field structures in the auroral acceleration region. Phys Rev Lett, 1997, 79: 1281–1284
4 Cattell C, Crumley J, Dombeck J, et al. Polar observations of solitary waves at the Earth's magnetopause. Geophys Res Lett, 2002, 29: 1065
5 Ergun R E, Andersson L, Main D S, et al. Parallel electric fields in the upward current region of the aurora: Indirect and direct observations. Phys Plasmas, 2002, 9: 3686–3694
6 Belhke R, Andre M, Bale S D, et al. Solitary structures associated with short large-amplitude magnetic structures (SLAMS) upstream of the Earth's quasi-parallel bow shock. Geophys Res Lett, 2004, 31: L16805
7 Deng X H, Tang R X, Matsumoto H, et al. Observations of electrostatic solitary waves associated with reconnection by geotail and cluster. Adv Space Res, 2006, 37: 1373–1381
8 Parks G K, Lee E, Mozer F, et al. Larmor radius size density holes discovered in the solar wind upstream of Earth's bow shock. Phys Plasmas, 2006, 13: 050701
9 Wilber M, Parks G K, Meziane K, et al. Foreshock density holes in the context of known upstream plasma structures. Ann Geophys, 2008, 26: 3741–3755
10 Washimi H, Taniuti T. Propagation of ion acoustic solitary waves of small amplitude. Phys Rev Lett, 1966, 17: 996–998
11 Ray D. Exact solitary ion acoustic waves in a magnetoplasma. Phys Fluids, 1979, 22: 2037–2038
12 Yu M Y, Shukla P K, Bujarbarua S. Fully nonlinear ion-acoustic solitary waves in a magnetized plasma. Phys Fluids, 1980, 23: 2146–2147
13 Lee L C, Kan J R. Nonlinear ion-acoustic waves and solitons in a magnetized plasma. Phys Fluids, 1981, 24: 430–433
14 Witt E, Lotko W. Ion-acoustic solitary waves in a magnetized plasma with arbitrary electron equation of state. Phys Fluids, 1983, 26: 2176–2185
15 Wu D J, Wang D Y, Falthammar C G. An analytical solution of finite-amplitude solitary kinetic Alfven waves. Phys Plasmas, 1995, 2: 4476–4481
16 Wu D J, Huang G L, Wang D Y. Solitary kinetic Alfven waves in the two-fluid model. Phys Plasmas, 1996, 3: 2879–2884
17 Wu D J, Wang D Y, Huang G L. Two dimensional solitary kinetic Alfven waves and dipole vortex structures. Phys Plasmas, 1997, 4: 611–617
18 Wei Y, Zong Q G, Pu Z Y, et al. Enhanced anti-sunward flow near local noon during a period of horizontal IMF and high solar wind velocity VY. Chin Sci Bull, 2011, 56: 1117–1122
19 Wang C R, Zong Q G, Wang Y F. Propagation of interplanetary shock excited ultra low frequency (ULF) waves in magnetosphere-ionosphere-atmosphere—Multi-spacecraft "cluster" and ground-based magnetometer observations. Sci China Tech Sci, 2010, 53: 2528–2534
20 Huang C, Wang R S, Lu Q M, et al. Electron density hole and quadruple structure of B_y during collisionless magnetic reconnection. Chin Sci Bull, 2010, 55: 718–722
21 Hull A J, Larson D E, Wilber M, et al. Large-amplitude electrostatic waves associated with magnetic ramp substructures at Earth's bow shock. Geophys Res Lett, 2006, 33: L15104
22 Hobara Y, Walker S N, Balikhin M, et al. Cluster observations of electrostatic solitary waves near the Eath's bow shock. J Geophys Res, 2008, 113: A05211